Supporting Information

Breath-Based SERS Detection of Propofol Metabolites during Anesthesia Using Mesoporous Au Foam Chips

Hui Zhang[1], Guanghui An[2], Enduo Feng[*1]

1. Shanghai Key Laboratory of Anesthesiology and Brain Functional Modulation, Clinical Research Center for Anesthesiology and Perioperative Medicine, Translational Research Institute of Brain and Brain-Like Intelligence, Shanghai Fourth People's Hospital, School of Medicine, Tongji University, Shanghai, 200434, China
2. Department of Anesthesiology, Shanghai General Hospital, Shanghai Jiao Tong University School of Medicine, Shanghai, 200080, China

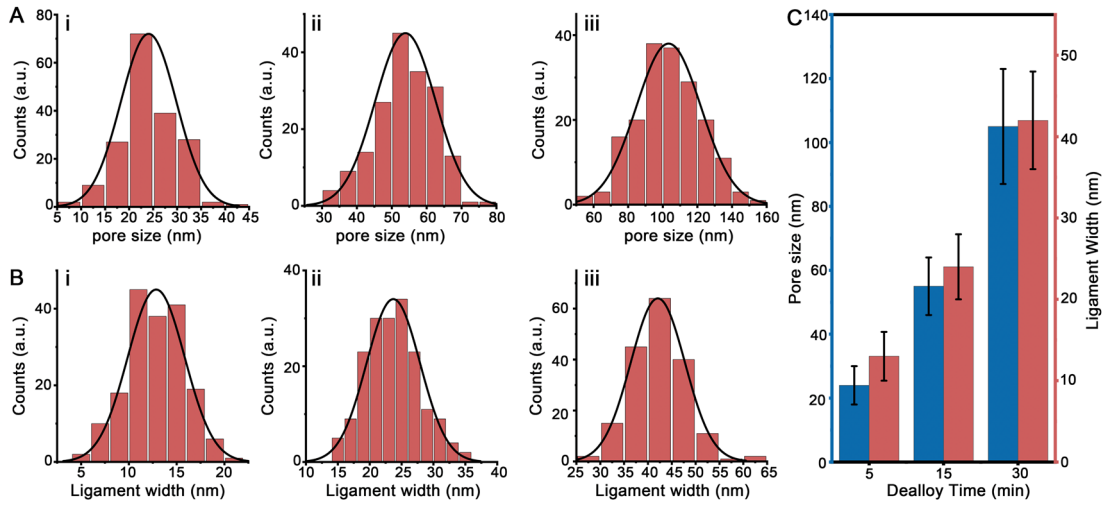

Figure S1. (A) Pore-size distributions of Au foam substrates dealloyed for (i) 5 min, (ii) 15 min, and (iii) 30 min. (B) Ligament-width distributions of Au foam substrates dealloyed for (i) 5 min, (ii) 15 min, and (iii) 30 min. (C) Summary of the average pore size and ligament width as a function of dealloying time.

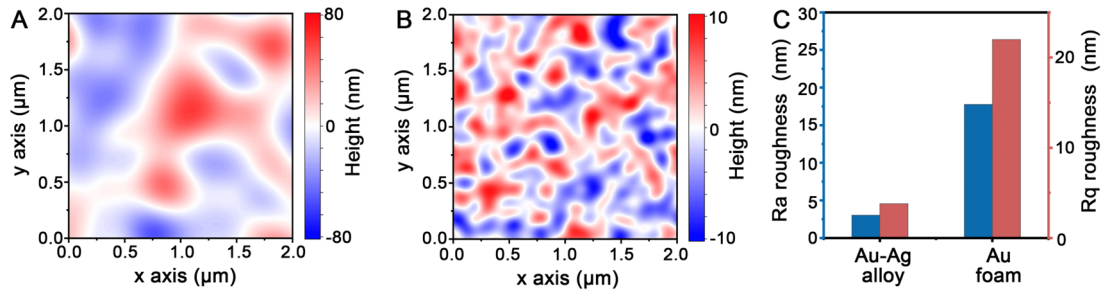

Figure S2. (A) AFM height image of the Au-Ag alloy precursor (B) AFM height image of the dealloyed Au foam substrate (C) Quantitative comparison of the arithmetic average roughness (Ra) and root-mean-square roughness (Rq) of the Au-Ag alloy and Au foam substrates.

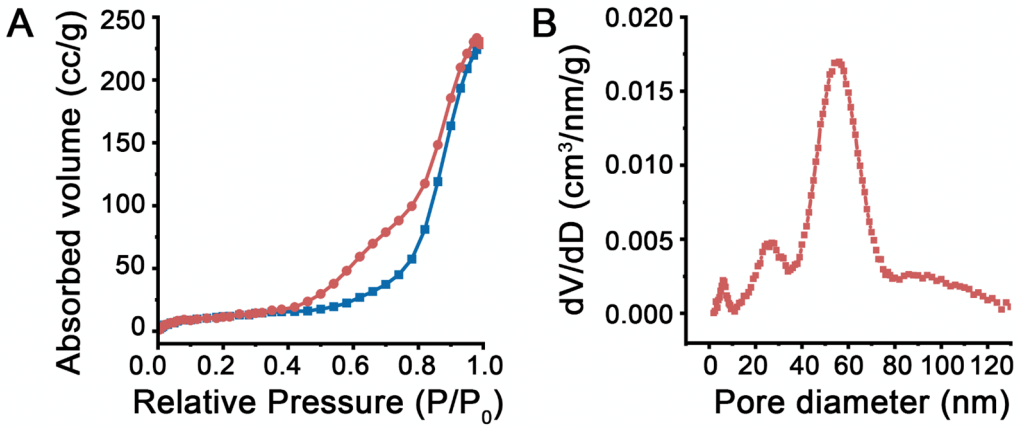

Figure S3. (A) Nitrogen adsorption–desorption isotherm of the optimized Au foam substrate measured at 77 K. (B) BJH pore-size distribution derived from the adsorption branch of the isotherm.

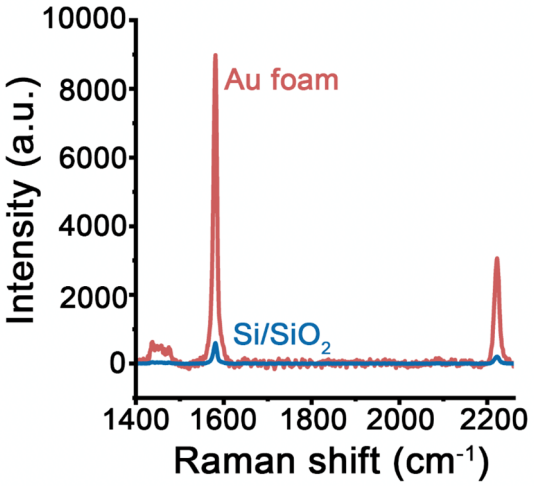

Figure S4. Representative Raman spectra of 4-MBN collected on Si/SiO_2 and the optimized Au foam substrate.

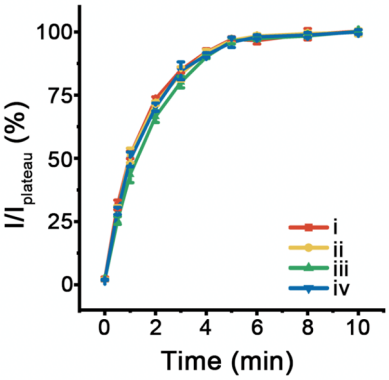

Figure S5. Response time of Au foam SERS platform for different metabolites of (i) propofol, (ii) 4-hydroxypropofol, (iii) propofol glucuronide, and (iv) propofol sulfate.

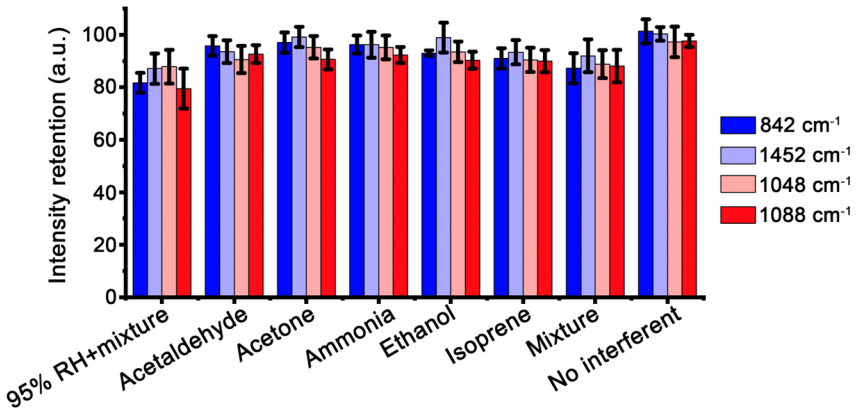

Figure S6. Signal retention of four selected Raman marker peaks, including 842, 1452, 1048, and 1088 cm^{-1}, under different breath-relevant interference conditions. The tested conditions included 95% RH with mixed interferents, acetaldehyde, acetone, ammonia, ethanol, isoprene, mixed interferents, and no-interferent control.

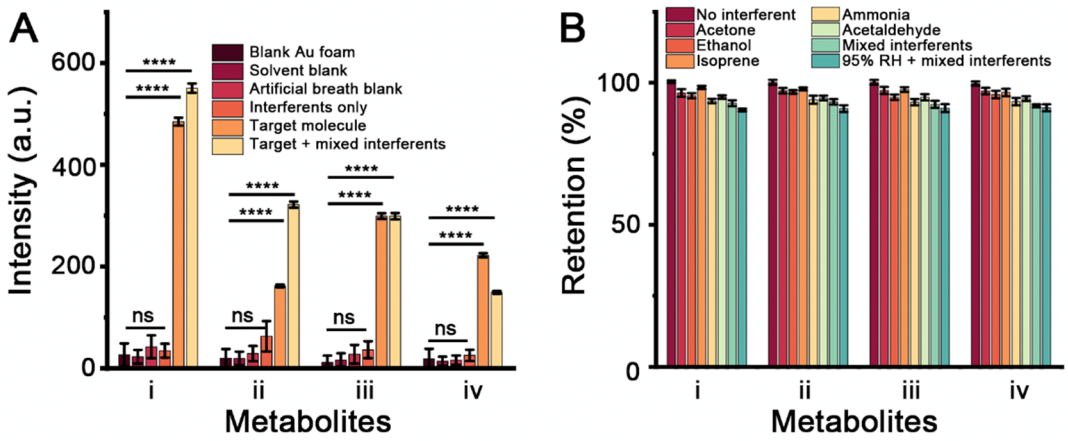

Figure S7. (A) Statistical comparison of marker-peak intensities under different control conditions, including blank Au foam, solvent blank, artificial breath blank, mixed interferents only, and target standards. (B) Signal retention of the selected marker peaks in the presence of individual or mixed breath-related interfering substances, including acetone, ethanol, isoprene, ammonia, acetaldehyde, mixed interferents, and 95% RH plus mixed interferents. Data are presented as mean ± SD, n=3. Statistical significance was determined by Student's t-test. *p < 0.05, **p < 0.01, ***p < 0.001, and ****p < 0.0001.

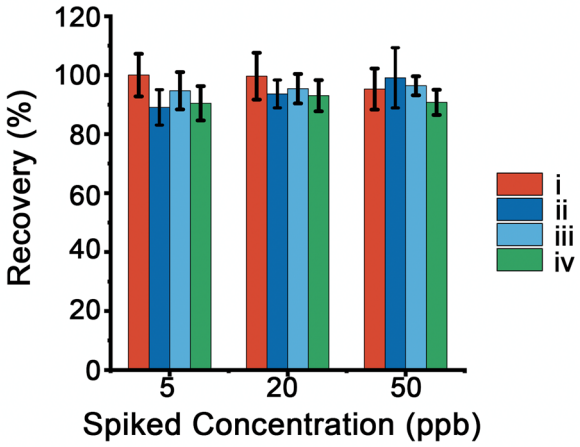

Figure S8. Spike-recovery results of four propofol-related molecules at different spiked concentrations of 5, 20, and 50 ppb in artificial breath matrix. i-iv correspond to propofol, 4-hydroxypropofol, propofol glucuronide, and propofol sulfate, respectively.

Table S1. Raman peak assignment of Propofol-related molecules.

Molecule	Peak / cm^{-1}	Peak assignment
Propofol	755	Aromatic ring deformation / isopropyl-related vibration
Propofol	1008	Aromatic ring breathing
Propofol	1178	Phenolic C–O stretching / C–H in-plane bending
Propofol	1266	C–O/C–H coupled vibration
Propofol	1452	Isopropyl C–H bending
Propofol	1602	Aromatic C=C stretching
4-Hydroxypropofol	842	Hydroxylation-sensitive aromatic ring deformation
4-Hydroxypropofol	1014	Aromatic ring breathing
4-Hydroxypropofol	1192	Phenolic C–O stretching
4-Hydroxypropofol	1284	C–O/C–H coupled vibration
4-Hydroxypropofol	1458	Isopropyl C–H bending
4-Hydroxypropofol	1608	Aromatic C=C stretching
Propofol glucuronide	1048	Glucuronide-associated C–O stretching
Propofol glucuronide	1122	C–O–C stretching
Propofol glucuronide	1170	C–O stretching / aromatic coupled vibration
Propofol glucuronide	1260	C–O/C–H coupled vibration
Propofol glucuronide	1342	Glucuronide-associated deformation vibration
Propofol glucuronide	1450	C–H bending
Propofol glucuronide	1600	Aromatic C=C stretching
Propofol sulfate	1088	S–O stretching
Propofol sulfate	1188	Sulfate-associated S=O/C–O coupled vibration
Propofol sulfate	1246	Sulfate/substituent-sensitive vibration
Propofol sulfate	1454	C–H bending
Propofol sulfate	1604	Aromatic C=C stretching

Table S2. The linear relationship parameter of four propofol-related molecules.

Molecule	Marker peak	Linear equation	R^2	LOD
Propofol	1452 cm^{-1}	I = 120.24C + 187.66	0.99977	0.847 ppb
4-Hydroxypropofol	842 cm^{-1}	I = 96.73C + 199.65	0.99987	0.663 ppb
Propofol glucuronide	1048 cm^{-1}	I = 78.43C + 301.85	0.99868	1.259 ppb
Propofol sulfate	1088 cm^{-1}	I = 88.59C + 248.91	0.99976	1.035 ppb

Table S3. Comparison of representative exhaled-breath propofol detection technologies.

Method	**Sensitivity**	**Selectivity**	**time**	**cost**	**Ref**
Real-time mass spectrometric breath analysis	High sensitivity	Moderate to high; based on ion signals	Real-time / rapid	High; requires mass spectrometric instrumentation	[1]
End-tidal propofol monitoring	Suitable for online clinical monitoring	Moderate; mainly targeted propofol signal	Online / near real-time	High; specialized analytical setup	[2]
Ion molecule reaction mass spectrometry	High	Moderate to high; ion-based detection	Rapid breath analysis	High; bulky MS-based platform	[3]
Ion mobility spectrometry	High	Moderate to high;	Rapid / online monitoring	Medium to high;	[4]
Online breath propofol monitoring	High	Targeted detection of breath propofol	Online / rapid	High; dedicated breath-analysis system	[5]
SESI-HRMS	High	Very high; high-resolution mass analysis enables broad molecular profiling	Rapid breath profiling	Very high; complex HRMS platform	[6]
Photoacoustic detection	High	Targeted optical detection	Real-time / rapid	Medium to high; requires specific photoacoustic detection system	[7]
This work: mesoporous Au foam SERS	LOD: 0.663-1.259 ppb; linear range: 2-75 ppb	Raman marker peaks; signal retention >90% under interference	5 min gas-phase exposure plus Raman readout	Relatively low; compact optical Raman platform	This work

[1] Harrison, G.R.; Critchley, A.D.J.; Mayhew, C.A.; Thompson, J.M. Real-Time Breath Monitoring of Propofol and Its Volatile Metabolites during Surgery Using a Novel Mass Spectrometric

Technique: A Feasibility Study. Br. J. Anaesth. 2003, 91, 797-799.
[2] Takita, A.; Masui, K.; Kazama, T. On-Line Monitoring of End-Tidal Propofol Concentration in Anesthetized Patients. Anesthesiology. 2007, 106, 659-664.
[3] Perl, T.; Carstens, E.; Hirn, A.; Quintel, M.; Vautz, W.; Nolte, J.; Jünger, M. Determination of Serum Propofol Concentrations by Breath Analysis Using Ion Molecule Reaction Mass Spectrometry. Br. J. Anaesth. 2009, 103, 822-827.
[4] Jiang, D.; Li, E.; Zhou, Q.; Wang, X.; Li, H.; Ju, B.; Guo, L.; Liu, D.; Li, H. Online Monitoring of Intraoperative Exhaled Propofol by Acetone-Assisted Negative Photoionization Ion Mobility Spectrometry Coupled with Time-Resolved Purge Introduction. Anal. Chem. 2018, 90, 5280-5289.
[5] Li, X.; Chang, P.; Zhang, W. Online Monitoring of Propofol Concentrations in Exhaled Breath. Heliyon. 2024, 10, e39704.
[6] Zeng, J.; Stankovic, N.; Singh, K.D.; Steiner, R.; Frey, U.; Erb, T.; Sinues, P. Breath Analysis of Propofol and Associated Metabolic Signatures: A Pilot Study Using Secondary Electrospray Ionization High-Resolution Mass Spectrometry. Anesthesiology. 2025, 143, 345-356.
[7] Meidert, A.S.; Rucz, P.; Angster, J.; Esser, J.; Miklós, A.; Schelling, G. Photoacoustic Detection of Propofol in Breath Gas for Monitoring Depth of Anaesthesia: From Bench to Bedside. Br. J. Anaesth. 2025, 135, 1203-1211.

Table S4. Basic clinical information and anesthesia protocol of patients enrolled for breath SERS analysis.

Patient ID	Age / years	Sex	Anesthesia protocol
P01	46	Male	Propofol-based general anesthesia
P02	52	Female	Propofol-based general anesthesia
P03	61	Male	Propofol-based general anesthesia
P04	55	Male	Propofol-based general anesthesia
P05	49	Male	Propofol-based general anesthesia
P06	67	Female	Propofol-based general anesthesia
P07	58	Male	Propofol-based general anesthesia
P08	44	Female	Propofol-based general anesthesia
P09	63	Male	Propofol-based general anesthesia
P10	70	Female	Propofol-based general anesthesia
P11	39	Female	Propofol-based general anesthesia
P12	56	Female	Propofol-based general anesthesia
P13	64	Male	Propofol-based general anesthesia
P14	47	Female	Propofol-based general anesthesia
P15	59	Male	Propofol-based general anesthesia
P16	73	Male	Propofol-based general anesthesia
P17	51	Female	Propofol-based general anesthesia
P18	68	Female	Propofol-based general anesthesia
P19	42	Male	Propofol-based general anesthesia
P20	60	Female	Propofol-based general anesthesia
P21	54	Male	Propofol-based general anesthesia
P22	65	Male	Propofol-based general anesthesia
P23	48	Male	Propofol-based general anesthesia
P24	57	Female	Propofol-based general anesthesia
P25	62	Female	Propofol-based general anesthesia
P26	50	Female	Propofol-based general anesthesia
P27	69	Male	Propofol-based general anesthesia
P28	45	Female	Propofol-based general anesthesia
P29	71	Male	Propofol-based general anesthesia
P30	53	Female	Propofol-based general anesthesia